Schizophrenia Research xxx (xxxx) xxx

Contents lists available at ScienceDirect

Schizophrenia Research

journal homepage: www.elsevier.com/locate/schres

Computational modeling of excitatory/inhibitory balance impairments in schizophrenia

Ning Qian [a], Richard M. Lipkin [a], Aleksandra Kaszowska [b], Gail Silipo [b], Elisa C. Dias [b], Pamela D. Butler [b], Daniel C. Javitt [b,c,*]

[a] Department of Neuroscience, Zuckerman Institute, Department of Physiology & Cellular Biophysics, Columbia University, New York, NY 10027, United States of America
[b] Schizophrenia Research Division, Nathan Kline Institute for Psychiatric Research, Orangeburg, NY 10962, United States of America
[c] Division of Experimental Therapeutics, Department of Psychiatry, Columbia University, New York, NY 10032, United States of America

ARTICLE INFO

Article history:
Received 12 January 2020
Received in revised form 16 March 2020
Accepted 17 March 2020
Available online xxxx

Keywords:
Contrast detection threshold
Adaptation
Recurrent model
Learning style

ABSTRACT

Deficits in glutamatergic function are well established in schizophrenia (SZ) as reflected in "input" dysfunction across sensory systems. By contrast, less is known about contributions of the GABAergic system to impairments in excitatory/inhibitory balance. We investigated this issue by measuring contrast thresholds for orientation detection, orientation discriminability, and orientation-tilt-aftereffect curves in schizophrenia subjects and matched controls. These measures depend on the amplitude and width of underlying orientation tuning curves, which, in turn, depend on excitatory and inhibitory interactions. By simulating a well-established V1 orientation selectivity model and its link to perception, we demonstrate that reduced cortical excitation *and* inhibition are *both* necessary to explain our psychophysical data. Reductions in GABAergic feedback may represent a compensatory response to impaired glutamatergic input in SZ, or a separate pathophysiological event. We also found evidence for the widely accepted, but rarely tested, inverse relationship between orientation discriminability and tuning width.

1. Introduction

Schizophrenia (SZ) is increasingly being viewed as a disease associated with widespread impairments in cortical excitatory-inhibitory balance (Lewis, 2009; Javitt and Sweet, 2015), potentially related to impaired function at *N*-methyl-D-aspartate receptors (NMDAR)-type glutamate receptors (Javitt et al., 2012; Javitt and Zukin, 1991; Kantrowitz and Javitt, 2012), as well as feedback dysregulation involving both parvalbumin and somatostatin-type GABAergic interneurons (Javitt et al., 2018; Dienel and Lewis, 2018). These deficits are manifest not only in higher cortical regions such as prefrontal cortex (Lewis, 2009), but also within sensory regions such as visual cortex, which can therefore be used to assess underlying neural mechanisms (Javitt and Freedman, 2014; Javitt, 2015).

In the present study, we investigated relative glutamatergic and GABA contributions to cortical information processing deficits in SZ using visual orientation processing as a model system. We compared SZ subjects and controls in two psychophysical experiments. First, we measured contrast threshold for detection of horizontally oriented gratings over a broad range of stimulus conditions (Fig. 1a). Since subjects had to distinguish between the presence and absence of a grating, this task depends primarily on orientation tuning amplitude, the difference between cells' peak firing to the presence of a grating and their baseline firing in the absence of a grating. The amplitude is determined by afferent glutamatergic drive from lateral geniculate nucleus (LGN) and recurrent excitation and inhibition within primary visual cortex (V1) (Butler et al., 2006; Martínez et al., 2012; Somers et al., 1995; Teich and Qian, 2003). Deficits in grating detection have been demonstrated using behavioral (Butler et al., 2001; Butler and Javitt, 2005), neurophysiological (Butler et al., 2006; Butler et al., 2005; Dias et al., 2011; Martínez et al., 2015; Schechter et al., 2005) and fMRI –based (Martínez et al., 2012; Martínez et al., 2008; Martínez et al., 2013) approaches.

Second, we measured orientation tilt aftereffect and the associated orientation discrimination (Fig. 1b). The tilt aftereffect is about how exposure to one (adaptor) orientation affects the perception of another (test) orientation. As such, it depends primarily upon orientation tuning width, which in turn depend on both excitatory drive and the pattern of recurrent glutamatergic and GABAergic connections within V1 according to computational models (Somers et al., 1995; Felsen et al., 2002; Ferster and Miller, 2000; Teich and Qian, 2003, 2006; Teich and Qian, 2010). At a circuit level (Ferster, 1986; Michalski et al., 1983), both

* Corresponding author at: Columbia University College of Physicians and Surgeons, 1051 Riverside Dr., Unit 21, New York, NY 10032, United States of America.
E-mail addresses: dcj2113@columbia.edu, javitt@nki.rfmh.org (D.C. Javitt).

https://doi.org/10.1016/j.schres.2020.03.027
0920-9964/

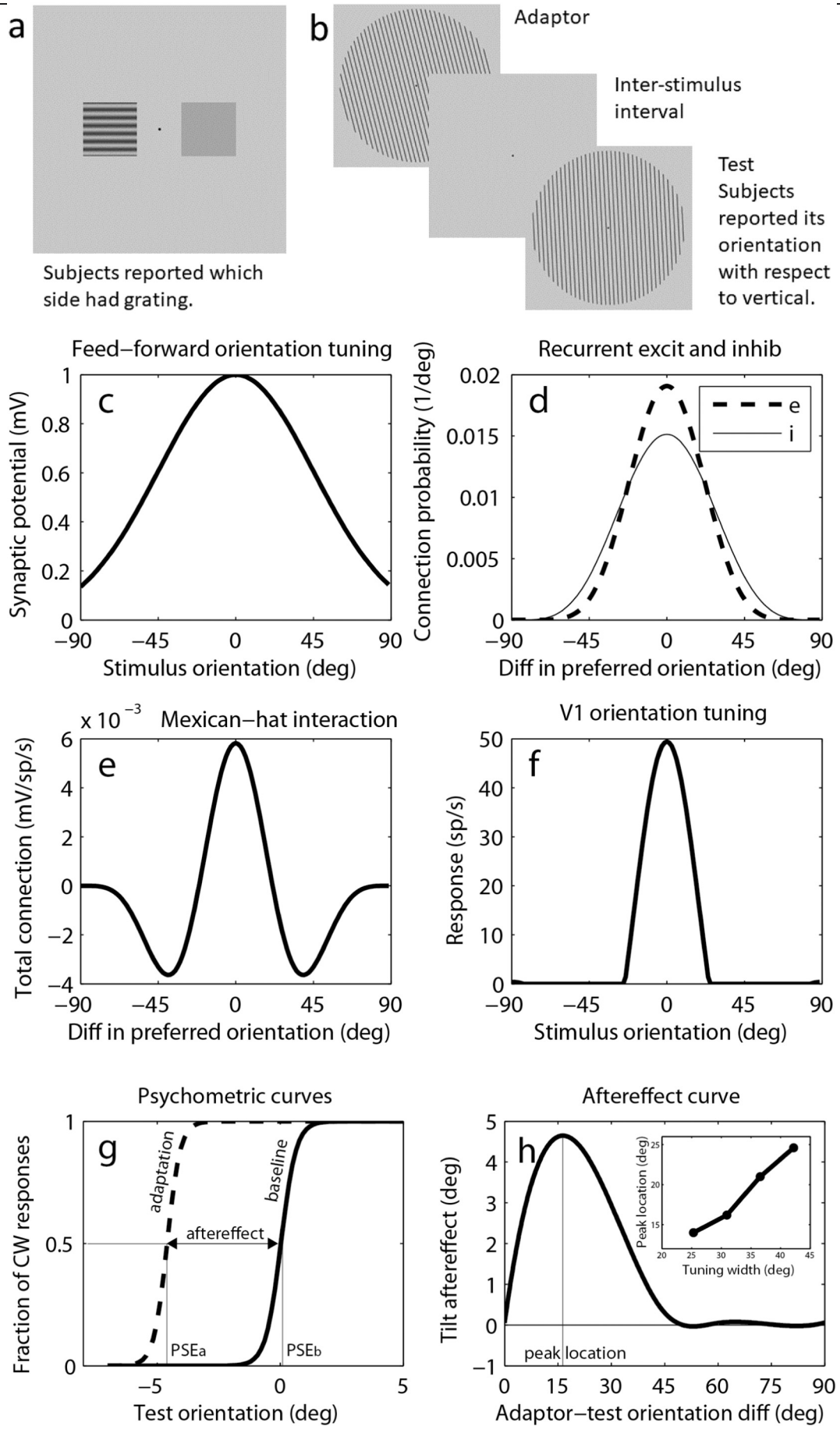

Please cite this article as: N. Qian, R.M. Lipkin, A. Kaszowska, et al., Computational modeling of excitatory/inhibitory balance impairments in schizophrenia, Schizophrenia Research, https://doi.org/10.1016/j.schres.2020.03.027

recurrent excitatory and inhibitory connections are strongest among cells with the same preferred orientation, and they drop off with increasing preferred-orientation difference. The models generally require that the inhibitory connectivity be wider than the excitatory connectivity (Fig. 1d), such that the net interaction among the V1 cells follows a center-excitation/surround-inhibition profile in the orientation domain (Fig. 1e), which can sharpen the weak feed-forward orientation bias into typical V1 orientation tuning curves (Fig. 1f) (Teich and Qian, 2010).

We used a range of test orientations around the vertical and asked subjects to report whether a given test orientation was clockwise (CW) or counterclockwise (CCW) relative to the vertical. A psychometric curve is the fraction of CW responses as a function of the test orientation (Fig. 1g). By comparing a subject's psychometric curve under an adaptation condition (Fig. 1g, dashed curve) with that under the baseline, no adaptation condition (Fig. 1g, solid curve), we measured the aftereffect. This aftereffect, as a function of the adaptor-test orientation difference (the "aftereffect curve," Fig. 1h), vanishes at 0° and 90° and peaks in-between (Gibson and Radner, 1937). The peak location depends on the range over which adaptor and test orientations produce overlapping neuronal firing patterns and thus indicates the underlying orientation tuning width (Fig. 1g, insert).

Orientation discriminability is measured by the slope at the mid-point of the psychometric curves, with steeper slopes indicating narrower tuning curves (Regan and Beverley, 1985; Lehky and Sejnowski, 1990; Zhang and Sejnowski, 1999; Abbott and Dayan, 1999; Teich and Qian, 2003).

Computational models have been developed to account for both the initial feedforward cortical responses to stimulus presentation shaped by the recurrent processes and for relating the responses to perceptual detection, discrimination, and aftereffects (Somers et al., 1995; Teich and Qian, 2003; Regan and Beverley, 1985; Zhaoping, 2014; Gilbert and Wiesel, 1990). Here, we measured grating detection and orientation discrimination/tilt aftereffects in independent patient cohorts and conducted computational modeling of both glutamatergic (excitatory) and GABAergic (inhibitory) component of processing. We hypothesized that contrast sensitivity for stimulus detection would be significantly reduced in SZ, particularly for magnocellular biased stimuli, reflecting NMDAR dysfunction within the subcortical and early cortical visual system. Although we had no strong a priori hypothesis regarding integrity of local GABAergic feedback, we hypothesized that use of computational modeling would permit assessment of the integrity of inhibitory processes relative to reductions in local excitatory drive.

2. Methods

2.1. Experiment 1: Contrast threshold for orientation detection

2.1.1. Subjects

We tested 24 (21 male) patients all meeting the Diagnostic and Statistical Manual of Mental Disorder (Fourth Edition) (DSM-IV) criteria for SZ (n = 21) or schizoaffective (n = 3) disorder; and 20 (16 male) healthy controls. Patients were recruited from inpatient (n = 8) and supervised residential care (n = 16) facilities associated with the Nathan Kline Institute (NKI), diagnosed using the Structured Clinical Interview for DSM-IV (SCID) and all available clinical data. Controls were recruited through NKI's Volunteer Recruitment Pool. Controls with a history of SCID-defined Axis I psychiatric disorder were excluded if they had any neurological or ophthalmologic disorders that might affect performance or met criteria for alcohol or substance dependence within the last 6 months or abuse within the last month. All participants provided informed consent according to the Declaration of Helsinki. This study was approved by NKI Institutional Review Board.

The groups did not differ significantly in age (patients: 37.7 ± 10.9; control 38.8 ± 12.1 years), gender (Fisher exact test, $p = 0.4$), or parental socioeconomic status (Hollingshead and Redlich, 1954) (patients: 40.5 ± 41.6; controls: 38.3 ± 14.2 $t_{34} = 0.2$, $p = 0.84$). All patients received antipsychotic medication. All subjects had 20/32 or better visual acuity (with or without correction) on the Logarithmic Visual Acuity Chart (Precision Vision, LaSalle, IL). For technical reasons, data were not obtained from 3 patients and 1 control in the 32-ms condition.

2.1.2. Apparatus

Stimuli were generated using the VENUS system (Neuroscientific Corporation, Farmingdale, NY) on a monitor (frame rate 119 Hz), subtending 5.7° x 5.7° of visual angle at a viewing distance of 150 cm. A chin rest and headboard stabilized participants' heads.

2.1.3. Luminance levels

Contrast sensitivity was measured at 5 luminance levels (0.01, 0.1, 1, 10, and 100 cd/m^2), achieved with Kodak Wratten Neutral Density Filter Gelatins 2.00 and 1.00 (two 2.00 filters; a 2.00 and a 1.00 filter; a 2.00 filter; a 1.00 filter; and no filters, respectively). The experiment progressed from lowest to highest luminance levels. Subjects were dark adapted for 20 min before testing and given 2-minute breaks between luminance levels to adapt to new lighting conditions.

2.1.4. Stimuli and procedures

Contrast sensitivity (CS), the inverse of contrast threshold, was measured with horizontal sine-wave gratings at 2 presentation durations (32- and 500-ms), 3 spatial frequencies (0.56, 4.47, and 11.18 cycles/deg), and 5 luminance levels (0.01, 0.1, 1, 10, and 100 cd/m^2), in a procedure described previously (Butler et al., 2005). Different conditions were run in randomized blocks with a spatial 2-alternative forced-choice paradigm. Gratings were presented randomly on either the monitor's right or left side; the opposing side uniformly displayed the same mean luminance (Fig. 1a). Participants indicated by keypad on which side they saw the grating. A 1-up-2-down staircase procedure measured participants' contrast threshold at 70.7% correct responses for each condition, using the mean of 10 reversals.

2.1.5. Data analysis

For the 32-ms duration, the 0.01 cd/m^2 luminance produced a floor effect: for both patients and controls, the staircases saturated at the highest contrast of one (i.e. contrast sensitivity of 1, Fig. 2). Thus, this luminance level is excluded from the analysis. A 2 Group (controls, patients) x 4 Luminance level (0.1, 1, 10, 100 cd/m^2) x 3 Spatial Frequency (0.56, 4.47, and 11.18 cycles/degree) mixed-design ANOVA was conducted. For the 500-ms duration, the same mixed-design ANOVA was conducted with 5 Luminance levels (0.01, 0.1, 1, 10, 100 cd/m^2). Appropriate post-hoc *t*-tests were applied when the ANOVA revealed significant main effects or interactions.

For each presentation duration and spatial frequency, we plotted contrast sensitivity as a function of mean luminance level. The resulting luminance gain functions were markedly non-linear for both patients and controls, with initial steep rise in slope, followed by plateau at high luminance; each luminance gain function was fitted with a Michaelis-Menten function.

Fig. 1. (a–b) The stimulus configurations for Experiments 1 and 2, respectively. (c–f) Recurrent model of orientation selectivity. (c) Broad, feedforward tuning. (d) Recurrent cortical excitatory (dashed) and inhibitory (dotted) connection probability as a function of the difference between cells' preferred orientations. (e) The center/surround recurrent interaction profile, with positive and negative values indicating net excitation and inhibition, respectively. (f) Sharp V1 tuning curve (for zero preferred orientation). (g) Schematic psychometric curves for the baseline condition (solid) and an adaptation condition (dashed). The test orientation for the mid-point of each condition is the perceived vertical or PSE. The difference between the PSE of an adaptation condition and that of the baseline condition is the aftereffect. The slope at PSE measures discriminability. (h) An aftereffect curve as a function of the adaptor-test orientation difference. The peak location is approximately proportional to tuning width (insert) when the tuning amplitude is kept constant.

Please cite this article as: N. Qian, R.M. Lipkin, A. Kaszowska, et al., Computational modeling of excitatory/inhibitory balance impairments in schizophrenia, Schizophrenia Research, https://doi.org/10.1016/j.schres.2020.03.027

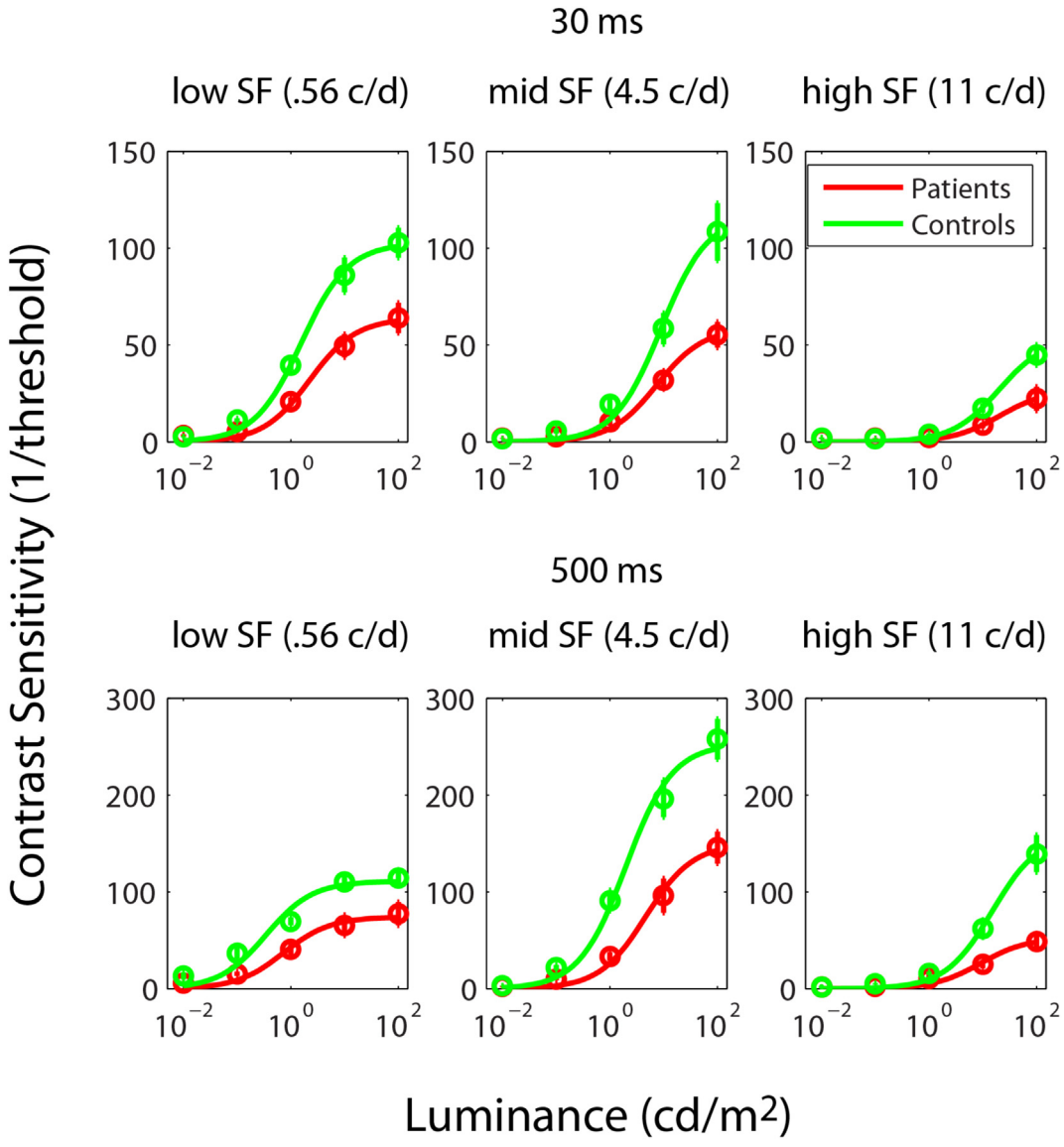

Fig. 2. Contrast sensitivity of orientation detection. Contrast sensitivity was measured over a variety of conditions for patients (red) and controls (green). The two rows show results from 32 ms and 500 ms presentation times, respectively. The three columns show results from 3 different spatial frequencies. Each panel plots contrast sensitivity as a function of luminance (in log scale). Error bars represent ± one standard error. (For interpretation of the references to colour in this figure legend, the reader is referred to the web version of this article.)

2.2. Experiment 2: Orientation discriminability and tilt aftereffect

2.2.1. Subjects

We tested 15 Sz patients and 14 controls, using the same criteria as in Experiment 1. The patient and control groups did not differ significantly in age (patients: 38.3 ± 10.7; controls: 39.8 ± 10.8 years, $t_{27} = -0.38$, $p = 0.71$], sex (Fisher's exact test, $p = 1.0$), or parental socioeconomic status (patients: 42.3 ± 12.1; controls: 47.3 ± 13.7, $t_{25} = -0.98$, $p = 0.34$).

2.2.2. Apparatus

The visual stimuli were presented on an Iiyama Vision Master Pro 514 monitor controlled by a PC computer. The vertical refresh rate was 85 Hz, and the spatial resolution was 1280 × 1024 pixels. The monitor was calibrated for linearity with a Minolta LS-110 photometer. In a dark room, subjects viewed the monitor at 54 cm distance, with a chin rest stabilizing head position. Each pixel subtended 0.035°. All experiments ran in Matlab with PsychToolbox 3 (Pelli, 1997; Brainard, 1997).

2.2.3. Visual stimuli

A round, black (0.01 cd/m^2) fixation dot, 0.35° in diameter, was shown at the center of the gray (74.7 cd/m^2) screen. All stimuli were black, anti-aliased line gratings (Qian and Dayan, 2013) covering a circular area 30° in diameter, with 0.11° wide lines evenly spaced and a center-to-center distance of 0.83°. Each grating's phase was randomly drawn from a uniform distribution over line spacing. We define vertical orientation as 0° and orientations CW and CCW from vertical as positive and negative angles, respectively.

2.2.4. Procedures

We used an orientation discrimination task to measure the tilt aftereffect as a function of the adaptor-test orientation difference (Fig. 1b). Each subject had 7 adaptation blocks, with 60 trials per block; each block's adapting grating had a fixed orientation of either 0°, −15°, −30°, −45°, −60°, −75°, or −90°; test gratings were a few degrees around vertical. Subjects initiated trial blocks by clicking a mouse button. The adapting grating appeared for 10 s in the first trial (initial adaptation) and 2 s in subsequent trials (top-up adaptation). After a 0.5 sec

Please cite this article as: N. Qian, R.M. Lipkin, A. Kaszowska, et al., Computational modeling of excitatory/inhibitory balance impairments in schizophrenia, Schizophrenia Research, https://doi.org/10.1016/j.schres.2020.03.027

inter-stimulus interval, a test stimulus appeared for 50 ms (Fig. 1b). Subjects then indicated by pressing right or left mouse button whether the test stimulus appeared to be CW or CCW, relative to vertical. After a 1-sec inter-trial interval, the next trial started. The test stimulus was selected according to a 1-up-1-down double staircase procedure: within each of two randomly interleaved staircases, the next test stimulus shifted one step more CW (CCW) if subjects' current response was CCW (CW). Each block lasted <5 min for both patients and controls. Subjects rested for at least 5 min after each adaptation block to avoid aftereffects carryover. We also ran a no-adaptation, baseline block, presenting only test stimuli. For each subject, the baseline block always ran first, followed by 7 adaptation blocks, ordered by either an increasing or decreasing sequence of adaptor orientations. The two sequences were counterbalanced within each subject group (for patients, 8 and 7 subjects ran the increasing and decreasing sequences, respectively). No performance feedback was given.

2.2.5. Data analysis

For each condition, the test stimuli were parameterized according to their orientations. Data were sorted to provide the fraction of CW responses to each test stimulus orientation; fractions were then plotted vs. test stimulus orientation. The resulting psychometric curve was fitted with a sigmoidal function whose mid-point indicated perceived vertical or point of subjective equality (PSE). An aftereffect is measured by the PSE difference between the adaptation condition and the corresponding baseline condition (the horizontal shift between the two curves' midpoints; Fig. 1g). The slope at PSE is a common measure of orientation discriminability: a steep (shallow) slope means that a subject is good (poor) at distinguishing two similar orientations.

One-way ANOVA was used to test the differences of aftereffect peak-locations and of slopes between patients and controls. Since we needed to measure both aftereffects and discriminability in Experiment 2, we plotted the data as psychometric curves to determine both PSEs and slopes, rather than using staircase reversals to determine PSEs only.

2.3. Computer simulations

For Experiment 1, we related tuning amplitude to contrast threshold. We considered N (20) cells tuned to the grating orientation. Their tuning amplitude as a function of the contrast is given by Albrecht and Hamilton (1982):

$$R_c = R_{\max}\frac{c^n}{c_{50}^n + c^n} + R_0 \quad (1)$$

where $R_{\max}$ is the maximum response amplitude (50 spikes/s from the recurrent model), R_0 is the background firing rate (1 spike/s), c is the contrast, c_{50} is the contrast where the amplitude is half maximum (0.2), and n is a power index that controls the saturation (1.5), all within the physiological ranges (Albrecht and Hamilton, 1982; Ringach et al., 2002; Qian and Andersen, 1995). For each of a set of contrasts, we used a noise model to simulate the percent-correct performance for distinguishing the presence vs. absence of a grating in the same way as in Teich and Qian (2003). Finally, we interpolated to determine the threshold as the contrast that produced a 70.7% correct performance, the same threshold definition in Experiment 1.

For Experiment 2, computer simulations were created by using a recurrent model for orientation selectivity (Teich and Qian, 2003). It considers oriented V1 cells with M (128) preferred orientations evenly distributed in the 180° range, receiving weakly orientation-biased feedforward excitatory inputs (Fig. 1c), which is sharpened by local feedback (Fig. 1d) according to a center-excitatory/surround-inhibitory connectivity pattern in the orientation domain (Fig. 1e).

We simulated tuning curves using parameters from Teich and Qian (2003) except the following modifications: $a_e = 3.5$, $a_i = 2.1$, $J_f^o = 1$, $J_e^o = 1.2$ and $J_i^o = 1.24$. The first two parameters determine the ranges of recurrent excitatory and inhibitory connections, respectively, whereas the last three determine the strengths of feedforward, recurrent excitatory, and recurrent inhibitory connections, respectively. They produced full tuning width at half height of 31°, well within the observed range (Ringach et al., 2002; Schiller et al., 1976). The tuning amplitude was the same as in Teich and Qian (2003) for high contrast gratings.

Finally, we simulated adaptation by reducing the excitatory recurrent connections around the adapted orientation (Teich and Qian, 2003) determined by parameter A_e, using a default measure of 0.00225 to match the controls' peak aftereffects. To simulate the psychometric function for each adaptor orientation and the baseline condition, we first ran the recurrent network to produce orientation tuning curves for all model cells, from which we read off their mean responses to each of a set of test orientations.

Then, we used the noise model of Teich and Qian (2003) to simulate the fraction of perceived orientation as CW to vertical where the perceived orientation is the population average of all cells. For the simulated psychometric curves, we determined the slopes, PSEs, and aftereffects, in the same way as our data analysis for Experiment 2.

2.3.1. Statistics

We compared two patient models, one with impaired excitation only, and the other with both impaired excitation and inhibition. After the parameters were chosen to match patients' tuning-width increase (Experiment 2), we used one-sample t-test to compare patients' tuning-amplitude reductions (Experiment 1, excluding the 0.01 cd/m^2 luminance conditions) with each model's predicted value. Relationships among variables were assessed using Pearson correlations. All statistics were two-tailed with preset alpha<0.05.

Some preliminary data of this study were reported previously in abstract form Qian et al. (2012).

3. Results

3.1. Experiment 1: Contrast threshold for orientation detection

For each subject and grating parameter set, we measured the contrast level needed to reach the 70.7% correct detection rate. The inverse of this contrast threshold is the contrast sensitivity. The data were analyzed separately for the short (32-ms) and long (500-ms) duration stimuli (Fig. 2), with between-subject factor of group membership (control/patient) and within-subject factors of luminance levels (0.1, 1, 10, 100 cd/m^2), and spatial frequencies (0.56, 4.47, and 11.18 cycles/degree), For the 32-ms duration, the 0.01 cd/m^2 luminance level was excluded due to floor effect. Across all luminance levels and spatial frequencies there was a highly significant main effect of group ($F_{1,40} = 17.2$, $p < 0.001$) indicating reduced contrast-sensitivity (increased detection threshold) in patients vs. controls. The mean effects of luminance ($F_{3,38} = 517$, $p < 0.001$) and spatial frequency ($F_{2,39} = 392$, $p < 0.001$) were also significant.

In addition, there were luminance x spatial-frequency interaction ($F_{6,35=}19.4$, $p < 0.001$), and a group x luminance x spatial-frequency interaction ($F_{6,35} = 2.69$, $p = 0.03$). The 3-way interaction indicates that group differences were affected by both luminance and spatial frequency. Patients showed a robust deficit at the scotopic luminance (0.1 cd/m^2) for 0.56 and 4.47 cyc/deg. frequencies (Fig. 1): the group differences were significantly greater for 0.56 and 4.47 cyc/deg. versus 11.18 cyc/deg. ($t_{18} = -5.85$ $p < 0.001$; $t_{18} = -3.23$, $p = 0.005$ respectively). For the higher luminance levels (1,10,100 cd/m^2), the group differences were similar across spatial frequencies ($p > 0.07$).

A similar three-way ANOVA was conducted for the 500-ms condition. All 5 luminance levels were included since the longer presentation duration alleviated the floor effect. There were main effects of group ($F_{1,40} = 25.6$, $p < 0.001$), spatial frequency ($F_{2,39} = 193.7$, $p < 0.001$), and luminance ($F_{4,37} = 187$, $p < 0.001$).

Please cite this article as: N. Qian, R.M. Lipkin, A. Kaszowska, et al., Computational modeling of excitatory/inhibitory balance impairments in schizophrenia, Schizophrenia Research, https://doi.org/10.1016/j.schres.2020.03.027

In addition, there were group x luminance ($F_{4,37} = 3.23$, $p = 0.023$), luminance x spatial-frequency ($F_{8,33} = 35.4$, $p < 0.001$), and group x luminance x spatial-frequency interactions ($F_{8,33} = 2.29$, $p = 0.045$), indicating that the group differences depend on luminance and spatial frequency. In follow-up analyses, patients again, showed a robust deficit in threshold under scotopic luminance conditions. The group difference at 0.01 cd/m^2 was significantly greater at 0.56 cyc/deg., and 4.47 cyc/deg. versus 11.18 c/deg. ($t_{19} = -2.84$, $p = 0.011$; $t_{19} = 3.9$, $p = 0.001$); and the difference at 4.47 cyc/deg. was larger versus 11.18 cyc/deg. ($t_{19} = -2.4$, $p = 0.006$).

In order to provide input to our computational models, we calculated mean contrast-sensitivity reduction across all conditions except those with 0.01 cd/m^2 luminance, resulting in a mean value of 46% (Fig. 2).

3.2. Experiment 2: Orientation tilt aftereffect and discriminability

For each subject and adaptation (or no-adaptation) condition, we measured whether a test grating in each trial was seen as CW or CCW relative to the vertical, and then plotted the fraction of trials with CW responses as a function of the test orientation. The resulting psychometric curves for controls and patients (see Suppl. Fig. 1 for examples) were used to calculate tilt aftereffects and peak locations of aftereffect curves (illustrated in Fig. 1g and h). The peak location (Fig. 3) was significantly greater for patients than controls, ($F_{1,27} = 4.48$, $p = 0.044$), demonstrating increased orientation tuning width. The patients' peak location was about 20% greater than that of the controls indicating a similar ratio of the two groups' tuning widths (Fig. 1h, insert). Consistent with the tuning-width increase, patients' orientation discriminability, as indicated by the slope of a psychometric function at PSE, was reduced compared with controls ($F_{1,27} = 7.43$, $p = 0.011$).

While it is generally accepted that orientation discriminability is inversely related to orientation tuning width, this theoretical notion has seldom been tested. Our study affords such a test because aftereffect peak location and the slope at PSE measure tuning width and discriminability, respectively. Fig. 3d shows that these two quantities indeed have a significant negative correlation (Pearson correlation coefficient $r = -0.54$, $p = 0.0028$).

3.3. Simulations: Impaired excitation and inhibition are both required to explain abnormal orientation processing in schizophrenia

Given patients' reduction of excitation observed in Experiment 1, we conducted simulation on the consequences of 1) adjusting excitation alone, or 2) combined excitation and inhibition (see Suppl. Fig. 2 for all the manipulations we tried). An adaptation parameter, reflecting reduction of recurrent excitation during adaptation, was also used to fit the data. Both the reduction of contrast sensitivity in Experiment 1 (46%) and the shift in peak aftereffect location in Experiment 2 (20%) were used to constrain the models.

For model 1 (excitation alone), we observed that to broaden tuning width by 20% by reducing excitation J_e^o alone required reducing tuning amplitude by >90%, thus predicting a reduction in contrast-sensitivity of 80%, vs. the observed 46%. The difference between values was highly significant ($t_{23} = 11.6$, $p = 4.2 \times 10^{-11}$).

By contrast, when both the recurrent excitation and inhibition strengths, J_e^o and J_i^o were reduced to 0.83 and 0.835, respectively, the tuning amplitude decreased by 60% to produce the observed 46% reduction of contrast sensitivity and the tuning width increased by 20% as desired. We used chi-square goodness-of-fit test of nested models to justify inhibition as an extra free parameter: With and without changing the inhibition parameter, the chi-square values are 0.86 and 15.9, respectively, and the difference between these values is highly significant ($\chi^2 = 15.04$, $df = 1$, $p = 0.0001$).

With the adjusted J_e^o and J_i^o, the adaptation parameter (A_e) of 0.006 produced a peak aftereffect comparable to that of the patients. The predicted aftereffect curve as a function of orientation difference (Fig. 3e),

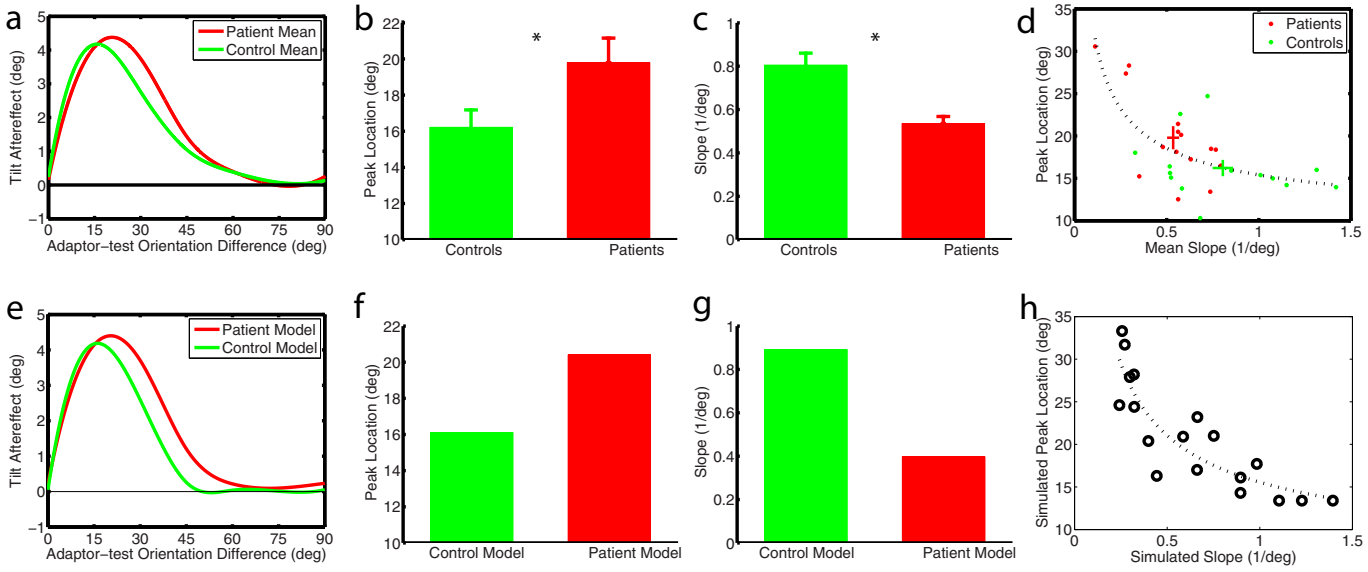

Fig. 3. Orientation discriminability and tilt aftereffect. (a–d) are psychophysical data and (e–h) are the corresponding simulation results. (a) The mean aftereffect curves for all the patients (red) and all the controls (green). (b) The peak locations of the aftereffect curves for the patient (red) and control (green) groups. The means and their standard errors are shown. As explained in the text, the peak location provides a robust measure of the underlying orientation tuning width. (c) The slopes of the psychometric functions for the patient (red) and control (green) groups. The means and their standard errors are shown. (d) The peak location of the aftereffect curve plotted against the mean slope of the psychometric functions. Each round dot represents an individual subject, red for the patients and green for the controls. The slopes from the 8 conditions (7 adaptation and 1 baseline) for each subject are averaged. The red and green crosses indicate the mean values for the patient and control groups, respectively. For each cross, the lengths of the vertical and horizontal lines represent 2 SEMs for the peak location and mean slope, respectively. The dotted curve is a power-function fit of all points. The simulation results in (e–h) are presented in similar format. In panel h, we varied the parameter set over a broad range; since there is no basis to classify a given parameter set as for control or patient, we plotted all points in black. (For interpretation of the references to colour in this figure legend, the reader is referred to the web version of this article.)

Please cite this article as: N. Qian, R.M. Lipkin, A. Kaszowska, et al., Computational modeling of excitatory/inhibitory balance impairments in schizophrenia, Schizophrenia Research, https://doi.org/10.1016/j.schres.2020.03.027

peak location (Fig. 3f) and slope at PSE (Fig. 3g) were highly similar to the observed ones (Fig. 3a–c).

Finally, we simulated the relationship between the aftereffect curve's peak location and psychometric curves' mean slope by covarying the three free parameters, constraining tuning amplitude to 10 to 70 spikes/s and aftereffect amplitude to 4 to 4.5 deg. The results, shown in Fig. 3h, has a negative correlation (Pearson correlation coefficient $r = -0.83$, $p = 0.000020$), similar to the data in Fig. 3d.

4. Discussion

We compared SZ and control subjects by measuring contrast thresholds for orientation detection to probe tuning amplitude, orientation discriminability and tilt aftereffect curve to probe glutamatergic/GABAergic balance in visual cortex in SZ. We found that patients had reduced contrast sensitivity specifically in magnocellular biased conditions, consistent with prior reports of reduced non-linear gain of feedforward excitation (Butler et al., 2006; Martínez et al., 2012), and also poorer orientation discriminability and broader tilt aftereffect curves (implying broader tuning widths).

Tuning amplitude and width depend on glutamate/GABA interactions, but in different ways, permitting use of pre-specified simulation approaches to probe relative glutamatergic and GABAergic dysfunction. We found that abnormal visual processing in SZ is best explained by reduced recurrent inhibition as well as excitation, supporting both GABAergic and glutamatergic contributions to impaired information processing in SZ.

In order to simulate the cortical changes associated with SZ, we modified 3 parameters (recurrent excitation, J_e^o; recurrent inhibition, J_i^o; and adaptation-induced reduction of recurrent excitation, A_e) of a previously published model for evaluation of orientation discriminability and tilt aftereffects (Teich and Qian, 2003). The best fit was obtained with a model that assumed smaller J_e^o and J_i^o, and a larger A_e, for the SZ patients compared with the controls.

A reduction of the recurrent excitation alone by 15% increased the tuning width by 20% as observed in SZ, but the amplitude was reduced too much (over 90%) resulting in significant discrepancies between modeled and observed contrast sensitivity impairment. By contrast, the final model, which assumed reductions in both excitation and inhibition produced behavioral parameters that were not significantly different from those observed in SZ, and was statistically superior ($p = 0.0001$) vs. the excitation alone model. We also varied these 3 parameters to simulate variations among the subjects (Fig. 3d vs. h), suggesting that the results may be applicable on a personalized basis to assess relative excitatory/inhibitory balance within individual subjects.

On a technical level, we observed a negative correlation between the slope of the psychometric function and the peak location of the tilt aftereffect curve. Since the peak location more directly measures underlying orientation tuning width, and the slope measures orientation discriminability, this finding supports the common, but little tested, theoretical prediction that orientation discriminability is inversely related to orientation tuning width (Regan and Beverley, 1985; Zhang and Sejnowski, 1999; Abbott and Dayan, 1999; Teich and Qian, 2003). We could test this prediction because our patients' and controls' data together covered a broad range of tuning width and discriminability.

A previous study also used an adaptation paradigm to show that SZ patients have broader orientation tuning than controls (Rokem et al., 2011). However, that study used the elevation of contrast detection threshold to measure tuning width, whereas we used a contrast detection task to measure tuning amplitude, and the orientation discriminability and tilt-aftereffect peak and as two measures of tuning width. Additionally, that study assumed impaired inhibition alone, which predicts an increased tuning amplitude, contradicting the patients' impaired contrast sensitivity (Fig. 2). By contrast, our study was guided by the well-known recurrent model of orientation selectivity. Constrained by the SZ and control subjects' data on contrast sensitivity, tilt aftereffect curve, and discriminability, our simulations suggest that both impaired cortical excitation and inhibition are important for understanding SZ behaviors.

Although the present study focused on orientation, SZ might have tuning deviations in other domains. For example, in the auditory system, SZ patients show reduced tone discrimination thresholds (Rabinowicz et al., 2000) and shallower categorical perceptual boundaries for speech sounds (Cienfuegos et al., 1999) that interrelated with impaired generation of NMDAR-dependent neurophysiological potentials such as mismatch negativity (MMN) (Javitt and Freedman, 2014; Javitt et al., 2000).

Similarly, in PFC NMDAR-related impairments in excitatory/inhibitory balance are postulated to underlie working memory deficits (Lewis, 2009). More generally, broader and weaker representations of information, such as those shown here in the visual system, could also lead to symptoms such as conceptual disorganization and thought disorder if present within high-level brain areas. In general, therefore, this study supports investigation of sensory brain regions as a means for investigating neural mechanisms implicated in generalized disturbances of excitatory/inhibitory balance in SZ.

The present findings are also consistent with neurochemical and post-mortem findings associated with schizophrenia. For example, Sz is associated with reductions in the width of the retinal nerve fiber layer and impaired electroretinographic activity(Lizano et al., 2020; Hebert et al., 2020; Silverstein et al., 2019), potentially contributing to input dysfunction. In addition reduced width (Reavis et al., 2017; Sprooten et al., 2013), volume (Dorph-Petersen et al., 2007), and total number of pyramidal neurons (Dorph-Petersen et al., 2007) has also been reported, consistent with glutamatergic dysfunction.

Reduction in GABA interneuron density, especially of somatostatin-type interneurons, are also reported for visual cortex (Tsubomoto et al., 2019) as have reductions in GABA concentration in visual cortex, as measured by MR spectroscopy, which correlate with impairments in orientation-specific surround suppression (Yoon et al., 2010). Physiological measures such as reduced visual P1 (Butler and Javitt, 2005; Schechter et al., 2005; Luck et al., 2006; Dias et al., 2013) or fMRI activation (Martínez et al., 2008) also suggest impaired excitatory/inhibitory balance within the early visual system.

In our study, all patients were receiving medication, which may also have affected local intracranial processing. However, the tilt-aftereffect has been investigated previously in Parkinson's disorder patients relative to SZ patients receiving depot antipsychotics (Calvert et al., 1991). Specifically, PD patients, in general, showed reduced tilt aftereffect when a high (10 cpd) stimulus spatial frequency and short test duration were used, opposite to the reported effects of L-dopa given to healthy individuals. Of note, however, no effects either of PD or of antipsychotics were noted at spatial frequencies and test durations similar to those used in the study.

In retina, activation of D1 receptors promotes, NMDAR dysfunction, suggesting a potential interplay between systems (Socodato et al., 2017). However, patterns of visual dysfunction in Sz are, in general, dissociable from those associated with dopaminergic abnormalities (Brandies and Yehuda, 2008). In addition to SZ patients, deficits in visual processing are also reported in unaffected first degree relatives (Yeap et al., 2006), as is reduced cortical thickness (Sprooten et al., 2013). Future studies of such individuals may therefore shed further light on underlying mechanisms without concern regarding medication confounds.

In summary, glutamatergic deficits in SZ are now well established and manifest in sensory input to cortex. Impaired glutamatergic drive, of its own, produces reduced GABAergic feedback due to lack of afferent drive. However, our results suggest that reductions in GABAergic local feedback are disproportionate to effects of glutamatergic deficits alone, and suggest a second, potentially compensatory reduction in GABAergic feedback within early sensory regions.

Please cite this article as: N. Qian, R.M. Lipkin, A. Kaszowska, et al., Computational modeling of excitatory/inhibitory balance impairments in schizophrenia, Schizophrenia Research, https://doi.org/10.1016/j.schres.2020.03.027

Contributors

NQ designed the orientation discrimination and tilt aftereffect studies, conducted computational modeling and wrote the initial draft of the manuscript.

RML advised on study design and data interpretation, and assisted in manuscript preparation.

AK implemented the orientation discrimination and tilt aftereffect paradigms, recruited and assessed subjects, and collected data.

GS supervised patient recruitment and characterization and coordinated assessment activities.

ECD supervised data collection for the orientation discrimination and tilt-aftereffect studies and assisted in manuscript preparation.

PDB designed and implemented the contrast sensitivity component of the study, supervised data collection and assisted in data interpretation and manuscript preparation.

DCJ had overall responsibility for study design and implementation, data analysis and interpretation and manuscript preparation.

Role of the funding source

NIH provided funding for patient recruitment, data collection, data analysis and manuscript preparation. The Simons Foundation and NSF provided funding to support computational modeling and manuscript preparation.

Declaration of competing interest

DCJ: Intellectual property for NMDAR agonists in schizophrenia, NMDAR antagonist in depression, fMRI for prediction of ECT response and ERP biomarkers for aging and schizophrenia. Equity in Glytech, AASI and NeuroRx. Scientific advisory board NeuroRx. Consultant payments Autifony, SK Life Sciences, Biogen, Cadence, and Pfizer.

Other authors report no conflicts.

Acknowledgements

Supported by USPHS grant MH49334 and MH109289 to DCJ; and a Simons Foundation Pilot grant 260653, and NSF grant 1754211 to NQ.

Appendix A. Supplementary data

Supplementary data to this article can be found online at https://doi.org/10.1016/j.schres.2020.03.027.

References

Abbott, L.F., Dayan, P., 1999. The effect of correlated variability on the accuracy of a population code. Neural Comput. 11 (1), 91–101.
Albrecht, D.G., Hamilton, D.B., 1982. Striate cortex of monkey and cat: contrast response function. J. Neurophysiol. 48 (1), 217–237.
Brainard, D.H., 1997. The psychophysics toolbox. Spat. Vis. 10, 433–436.
Brandies, R., Yehuda, S., 2008. The possible role of retinal dopaminergic system in visual performance. Neurosci. Biobehav. Rev. 32 (4), 611–656.
Butler, P.D., Javitt, D.C., 2005. Early-stage visual processing deficits in schizophrenia. Curr. Opin. Psychiatry 18 (2), 151–157.
Butler, P.D., Schechter, I., Zemon, V., Schwartz, S.G., Greenstein, V.C., Gordon, J., et al., 2001. Dysfunction of early-stage visual processing in schizophrenia. Am. J. Psychiatr. 158 (7), 1126–1133.
Butler, P.D., Zemon, V., Schechter, I., Saperstein, A.M., Hoptman, M.J., Lim, K.O., et al., 2005. Early-stage visual processing and cortical amplification deficits in schizophrenia. Arch. Gen. Psychiatry 62 (5), 495–504.
Butler, P.D., Martinez, A., Foxe, J.J., Kim, D., Zemon, V., Silipo, G., et al., 2006. Subcortical visual dysfunction in schizophrenia drives secondary cortical impairments. Brain 130 (2), 417–430.
Calvert, J.E., Harris, J.P., Phillipson, O.T., 1991. Tilt aftereffect reveals early visual processing deficits in Parkinson's disease and in chronic schizophrenic patients on depot neuroleptic. Psychopathology 24 (6), 375–380.
Cienfuegos, A., March, L., Shelley, A.-M., Javitt, D.C., 1999. Impaired categorical perception of synthetic speech sounds in schizophrenia. Biol. Psychiatry 45 (1), 82–88.
Dias, E.C., Butler, P.D., Hoptman, M.J., Javitt, D.C., 2011. Early sensory contributions to contextual encoding deficits in schizophrenia. Arch. Gen. Psychiatry 68 (7), 654–664.
Dias, E.C., Bickel, S., Epstein, M.L., Sehatpour, P., Javitt, D.C., 2013. Abnormal task modulation of oscillatory neural activity in schizophrenia. Front. Psychol. 4, 540.
Dienel, S.J., Lewis, D.A., 2019. Alterations in cortical interneurons and cognitive function in schizophrenia. Neurobiol. Dis. 131, 104208.
Dorph-Petersen, K.A., Pierri, J.N., Wu, Q., Sampson, A.R., Lewis, D.A., 2007. Primary visual cortex volume and total neuron number are reduced in schizophrenia. J. Comp. Neurol. 501 (2), 290–301.
Felsen, G., Shen, Y.S., Yao, H., Spor, G., Li, C., Dan, Y., 2002. Dynamic modification of cortical orientation tuning mediated by recurrent connections. Neuron 36 (5), 945–954.
Ferster, D., 1986. Orientation selectivity of synaptic potentials in neurons of cat primary visual cortex. J. Neurosci. 6 (5), 1284–1301.
Ferster, D., Miller, K.D., 2000. Neural mechanisms of orientation selectivity in the visual cortex. Annu. Rev. Neurosci. 23, 441–471.
Gibson, J.J., Radner, M., 1937. Adaptation, after-effect and contrast in the perception of tilted lines. I. Quantitative studies. J. Exp. Psychol. 20, 453–467.
Gilbert, C.D., Wiesel, T.N., 1990. The influence of contextual stimuli on the orientation selectivity of cells in primary visual cortex of the cat. Vis. Res. 30 (11), 1689–1701.
Hebert, M., Merette, C., Gagne, A.M., Paccalet, T., Moreau, I., Lavoie, J., et al., 2020. The electroretinogram may differentiate schizophrenia from bipolar disorder. Biol. Psychiatry 87 (3), 263–270.
Hollingshead, A.B., Redlich, F., 1954. Schizophrenia and social structure. Am. J. Psychiatr. 110 (9), 695–701.
Javitt, D.C., 2015. Neurophysiological models for new treatment development in schizophrenia: early sensory approaches. Ann. N. Y. Acad. Sci. 1344, 92.
Javitt, D.C., Freedman, R., 2014. Sensory processing dysfunction in the personal experience and neuronal machinery of schizophrenia. Am. J. Psychiatr. 172 (1), 17–31.
Javitt, D.C., Sweet, R.A., 2015. Auditory dysfunction in schizophrenia: integrating clinical and basic features. Nat. Rev. Neurosci. 16 (9), 535.
Javitt, D.C., Zukin, S.R., 1991. Recent advances in the phencyclidine model of schizophrenia. Am. J. Psychiatr. 148 (10), 1301–1308.
Javitt, D.C., Shelley, A.-M., Ritter, W., 2000. Associated deficits in mismatch negativity generation and tone matching in schizophrenia. Clin. Neurophysiol. 111 (10), 1733–1737.
Javitt, D.C., Zukin, S.R., Heresco-Levy, U., Umbricht, D., 2012. Has an angel shown the way? Etiological and therapeutic implications of the PCP/NMDA model of schizophrenia. Schizophr. Bull. 38 (5), 958–966.
Javitt, D.C., Lee, M., Kantrowitz, J.T., Martinez, A., 2018. Mismatch negativity as a biomarker of theta band oscillatory dysfunction in schizophrenia. Schizophr. Res. 191, 51–60.
Kantrowitz, J., Javitt, D.C., 2012. Glutamatergic transmission in schizophrenia: from basic research to clinical practice. Curr. Opin. Psychiatry 25 (2), 96.
Lehky, S.R., Sejnowski, T.J., 1990. Neural model of stereoacuity and depth interpolation based on a distributed representation of stereo disparity.[erratum appears in J Neurosci 1991 Mar;11(3):followi]. J. Neurosci. 10 (7), 2281–2299.
Lewis, D.A., 2009. Neuroplasticity of excitatory and inhibitory cortical circuits in schizophrenia. Dialogues Clin. Neurosci. 11 (3), 269.
Lizano, P., Bannai, D., Lutz, O., Kim, L.A., Miller, J., Keshavan, M., 2020. A meta-analysis of retinal cytoarchitectural abnormalities in schizophrenia and bipolar disorder. Schizophr. Bull. 46 (1), 43–53.
Luck, S.J., Fuller, R.L., Braun, E.L., Robinson, B., Summerfelt, A., Gold, J.M., 2006. The speed of visual attention in schizophrenia: electrophysiological and behavioral evidence. Schizophr. Res. 85 (1–3), 174–195.
Martínez, A., Hillyard, S.A., Dias, E.C., Hagler, D.J., Butler, P.D., Guilfoyle, D.N., et al., 2008. Magnocellular pathway impairment in schizophrenia: evidence from functional magnetic resonance imaging. J. Neurosci. 28 (30), 7492–7500.
Martínez, A., Hillyard, S.A., Bickel, S., Dias, E.C., Butler, P.D., Javitt, D.C., 2012. Consequences of magnocellular dysfunction on processing attended information in schizophrenia. Cereb. Cortex 22 (6), 1282–1293.
Martínez, A., Revheim, N., Butler, P.D., Guilfoyle, D.N., Dias, E.C., Javitt, D.C., 2013. Impaired magnocellular/dorsal stream activation predicts impaired reading ability in schizophrenia. NeuroImage: Clin. 2, 8–16.
Martínez, A., Gaspar, P.A., Hillyard, S.A., Bickel, S., Lakatos, P., Dias, E.C., et al., 2015. Neural oscillatory deficits in schizophrenia predict behavioral and neurocognitive impairments. Front. Hum. Neurosci. 9, 371.
Michalski, A., Gerstein, G.L., Czarkowska, J., Tarnecki, R., 1983. Interactions between cat striate cortex neurons. Exp. Brain Res. 51 (1), 97–107.
Pelli, D.G., 1997. The VideoToolbox software for visual psychophysics: transforming numbers into movies. Spat. Vis. 10, 437–442.
Qian, N., Andersen, R.A., 1995. V1 responses to transparent and nontransparent motions. Exp. Brain Res. 103 (1), 41–50.
Qian, N., Dayan, P., 2013. The company they keep: background similarity influences transfer of aftereffects from second- to first-order stimuli. Vis. Res. 87, 35–45.
Qian, N., Lipkin, R.M., Kaszowska, A., Dias, E.C., Javitt, D.C., 2012. Schizophrenia and Autism as Opposite Tuning-Function Disorders: A theory2012: Program No. 772.11, 2012 Neuroscience Meeting Planner. Society for Neuroscience, New Orleans, LA (Online).
Rabinowicz, E.F., Silipo, G., Goldman, R., Javitt, D.C., 2000. Auditory sensory dysfunction in schizophrenia: imprecision or distractibility? Arch. Gen. Psychiatry 57 (12), 1149–1155.
Reavis, E.A., Lee, J., Wynn, J.K., Engel, S.A., Jimenez, A.M., Green, M.F., 2017. Cortical thickness of functionally defined visual areas in schizophrenia and bipolar disorder. Cereb. Cortex 27 (5), 2984–2993.
Regan, D., Beverley, K.I., 1985. Postadaptation orientation discrimination. J. Opt. Soc. Am. A Opt. Image Sci. 2 (2), 147–155.
Ringach, D.L., Shapley, R.M., Hawken, M.J., 2002. Orientation selectivity in macaque V1: diversity and laminar dependence. J. Neurosci. 22 (13), 5639–5651.
Rokem, A., Yoon, J.H., Ooms, R.E., Maddock, R.J., Minzenberg, M.J., Silver, M.A., 2011. Broader visual orientation tuning in patients with schizophrenia. Front. Hum. Neurosci. 5.
Schechter, I., Butler, P.D., Zemon, V.M., Revheim, N., Saperstein, A.M., Jalbrzikowski, M., et al., 2005. Impairments in generation of early-stage transient visual evoked potentials to magno-and parvocellular-selective stimuli in schizophrenia. Clin. Neurophysiol. 116 (9), 2204–2215.
Schiller, P.H., Finlay, B.L., Volman, S.F., 1976. Quantitative Studies of Single-Cell Properties in Monkey Striate Cortex. II. Orientation Specificity and Ocular Dominance (1976-11-01 00:00:00. 1320-33 p).
Silverstein, S.M., Fradkin, S.I., Demmin, D.L., 2019. Schizophrenia and the retina: towards a 2020 perspective. Schizophr. Res. https://doi.org/10.1016/j.schres.2019.09.016.

Please cite this article as: N. Qian, R.M. Lipkin, A. Kaszowska, et al., Computational modeling of excitatory/inhibitory balance impairments in schizophrenia, Schizophrenia Research, https://doi.org/10.1016/j.schres.2020.03.027

Socodato, R., Santiago, F.N., Portugal, C.C., Domith, I., Encarnacao, T.G., Loiola, E.C., et al., 2017. Dopamine promotes NMDA receptor hypofunction in the retina through D1 receptor-mediated Csk activation, Src inhibition and decrease of GluN2B phosphorylation. Sci. Rep. 7, 40912.

Somers, D.C., Nelson, S.B., Sur, M., 1995. An emergent model of orientation selectivity in cat visual cortical simple cells. J. Neurosci. 15 (8), 5448–5465.

Sprooten, E., Papmeyer, M., Smyth, A.M., Vincenz, D., Honold, S., Conlon, G.A., et al., 2013. Cortical thickness in first-episode schizophrenia patients and individuals at high familial risk: a cross-sectional comparison. Schizophr. Res. 151 (1–3), 259–264.

Teich, A.F., Qian, N., 2003. Learning and adaptation in a recurrent model of V1 orientation selectivity. J. Neurophysiol. 89 (4), 2086–2100.

Teich, A.F., Qian, N., 2006. Comparison among some models of orientation selectivity. J. Neurophysiol. 96 (1), 404–419.

Teich, A.F., Qian, N., 2010. V1 orientation plasticity is explained by broadly tuned feedforward inputs and intracortical sharpening. Vis. Neurosci. 27 (1–2), 57–73.

Tsubomoto, M., Kawabata, R., Zhu, X., Minabe, Y., Chen, K., Lewis, D.A., et al., 2019. Expression of transcripts selective for GABA neuron subpopulations across the cortical visuospatial working memory network in the healthy state and schizophrenia. Cereb. Cortex 29 (8), 3540–3550.

Yeap, S., Kelly, S.P., Sehatpour, P., Magno, E., Javitt, D.C., Garavan, H., et al., 2006. Early visual sensory deficits as endophenotypes for schizophrenia: high-density electrical mapping in clinically unaffected first-degree relatives. Arch. Gen. Psychiatry 63 (11), 1180–1188.

Yoon, J.H., Maddock, R.J., Rokem, A., Silver, M.A., Minzenberg, M.J., Ragland, J.D., et al., 2010. GABA concentration is reduced in visual cortex in schizophrenia and correlates with orientation-specific surround suppression. J. Neurosci. 30 (10), 3777–3781.

Zhang, K.C., Sejnowski, T.J., 1999. Neuronal tuning: to sharpen or broaden? Neural Comput. 11 (1), 75–84.

Zhaoping, L., 2014. Understanding Vision: Theory, Models, and Data. Oxford University Press, London, UK.

Please cite this article as: N. Qian, R.M. Lipkin, A. Kaszowska, et al., Computational modeling of excitatory/inhibitory balance impairments in schizophrenia, Schizophrenia Research, https://doi.org/10.1016/j.schres.2020.03.027